Magazine of Civil Engineering

ISSN 2712-8172

journal homepage: http://engstroy.spbstu.ru/

DOI: 10.34910/MCE.108.1

Interaction and control measures of shallow-buried shield twin tunnels with small clear-distance

S.H. Liu [a], ***Y. Shi*** [b], ***Y.D. Zhao**** [a, c], ***R. Sun*** [a]

[a] *Central South University, Changsha City, Hunan Province, China*

[b] *Cccc Second Harbour Eingineering Company Design & Research Institute Co., Wuhan, China*

[c] *School of Civil Engineering, Yancheng Institute of Technology, Yancheng City, Jiangsu Province, China*

**E-mail: y.d.zhao@ycit.edu.cn*

Keywords: earth pressure balance (EPB) shield, twin tunnels, tunnelling interaction, finite element method, ABAQUS, testing

Abstract. When constructing small clear-distance tunnels in complex geotechnical conditions, there are many challenges including intolerable ground movement, face failure, and potential damage to adjacent tunnel. This paper focused on the study of small clear-distance shield tunnel construction in the typical upper-soft and lower-hard stratum. Numerical analyses are conducted to estimate the influence of the new tunneling on the existing tunnel. In addition, partition wall accompanied by cement-soil mixing pile is adopted as the control measure. The results demonstrate that the construction of the new tunnel has a big impact on the stability of the existing tunnel. The seal roof block should not be placed on the top region. The obviously influenced region of the existing tunnel agrees with the excavation diameter of the new tunnel, so monitoring in this region should be strengthened. Moreover, the safety control effect has been verified by numerical analysis and field test. This study provides a basis for the design and construction of tunnels with shallow buried depths and small clear-distances.

1. Introduction

With the development of urban metro network, many shield twin tunnels with small clear-distances have been excavated in shallow strata [1–4]. However, previous studies have shown that tunneling construction often significantly affects the existing tunnel structure [5–10] and the excavation of a tunnel in a shallow stratum can lead to the collapse of the tunnel face and overlarge surface subsidence [11–14]. Construction of such tunnels may incur severe accidents because of high construction difficulty and risk.

The interaction mechanism of shallow-buried or small clear-distance shield twin tunnels is a significant issue that has aroused the interest of many investigators. Many researchers have carried out analytical studies [15–19], model tests [20–22], field tests [23–27] and numerical simulations [28–33] to study the interaction mechanisms of shallow-buried or small clear-distance shield twin tunnels. Among them, numerical simulation is usually used in the analysis of shield tunnelling as an efficient and low-cost method. Three-dimensional finite element calculation [5] was presented to investigate the effect of tunneling on an adjacent tunnel. The interaction between two parallel tunnels was investigated through a series of numerical simulations [30]. Another numerical model [6] was presented to evaluate ground displacement surrounding the two tunnels. The finite element method was used to explore the influence of the relative position of two circular tunnels on the soil movement and to examine the internal forces in the lining [5]. A numerical model [31] was presented to evaluate the face stability of a shallow-shield tunnel. The collapse mechanism [19, 32] was presented to investigate the face stability of a shallow tunnel. The discrete element method [33] was used to investigate the face stability analysis of shallow shield tunnels. However, few

Liu, S.H., Shi, Y., Zhao, Y.D., Sun, R. Interaction and control measures of shallow-buried shield twin tunnels with small clear-distance. Magazine of Civil Engineering. 2021. 108(8). Article No. 10801. DOI: 10.34910/MCE.108.1

publications have concentrated on the interaction mechanism of shallow-buried shield twin tunnels with small clear-distance. Consequently, the interaction mechanism of shallow-buried shield twin tunnels with small clear-distance needs to be further studied so as to provide an accurate basis for effective control measures of the tunnel. The objects of research are listed as following, 1. deformation of the ground surface; 2. mechanical responses of the first tunnel; 3. reasonable control measures under the condition of shallow-buried twin tunnels with small clear-distance. For this reason, and the goals of the research is listed as following are listed as following, 1. acquiring the settlement troughs; 2. calculating the displacement and internal force of tunnel; 3. comparing the opening status; 4. verifying the effectiveness of control measures.

In this paper, considering the effect of the segment joint, a three-dimensional numerical model of the shield tunnel segment is established based on practical engineering, and the interaction of shallow-buried twin tunnels with small clear-distance is studied. In addition, an effective control measure is applied to the field, which can be verified as an effective method not only by numerical results but also by field tests.

2. Methods

2.1. Formulation of the problem

The main route of the intercity railway tunnel 2, which at Chencun, Guangzhou, between the 'Chencun' station in the south and the 'Guangzhou South' station in the Southern part of the city, consists of two tubes 8.5 m in external diameter and 3969 m in length. Two EPBs are working to excavate the twin tunnels. The tunnel segment is made of C50 concrete, with an external diameter of 8.5 m, a thickness of 0.4 m and a width of 1.6 m. Moreover, M30 high-strength bolts are used for circumferential and longitudinal connections of the tunnel segments. The principal strata, where the twin tunnels are situated, is comprised of silt, fine sand, strongly weathered mudstone and weathered mudstone, as shown in Fig. 1. Note that the clear-distance between these tunnels is 3.1 m and burial depth is 5.5 m within the region of shield launching. The construction procedure of the twin tunnels is that the first tunnel (existing tunnel) has been completed before the construction of the second tunnel (new tunnel).

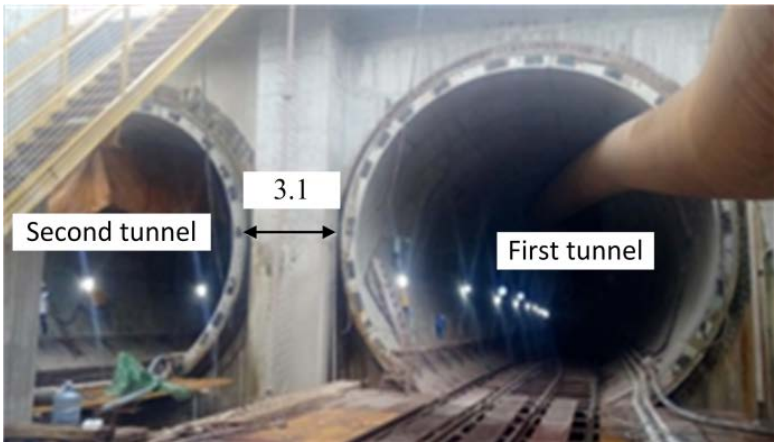

Figure 1(a). Profile of the tunnel: Condition of the launching shaft (Unit: m).

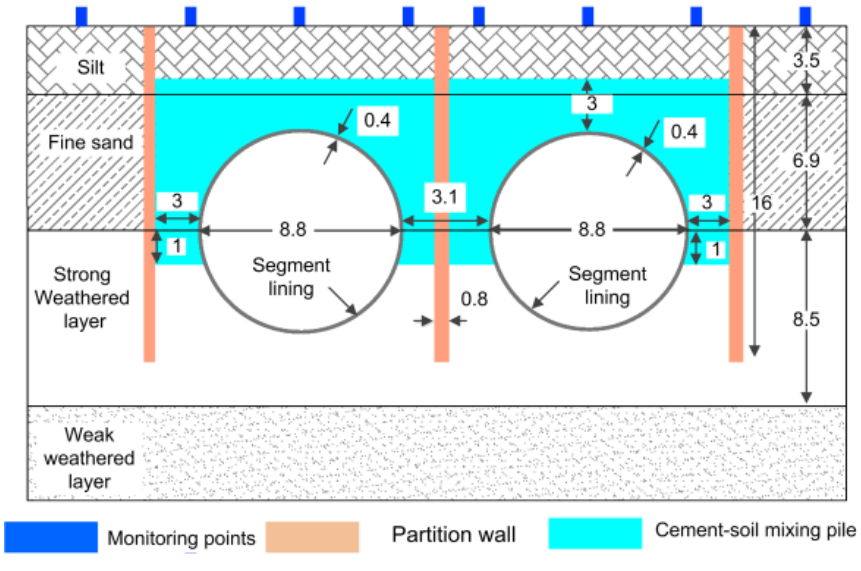

Figure 1(b). Profile of the tunnel: Geological condition (Unit: m).

In view of the aforementioned conditions around the tunnels, the tunneling work in this area is faced with such challenges as upper-soft and lower-hard stratum, shallow burial depth, and small clear-distance. Therefore, the stability of the first tunnel, which might be influenced by the tunneling of the second one, must be ensured to keep the safety of the whole transport line and the surrounding environment.

2.2. Method for solving the problem

Numerical simulation [5, 7, 8, 28–33, 35] is a commonly-used reliable method for the evaluation and investigation of civil engineering projects because it has the advantages of data visualization, high speed of solution and low cost. Finite Element Method (FEM) is applied in this paper to accurately analyze the influence mechanism between these shield tunnels. Partition wall accompanied by cement-soil mixing pile (Fig. 1 and Fig. 2) is adopted as the control measure for ensuring the safety of the tunneling. The pre-reinforcement range of cement-soil mixing piles is 26.7 m (X) × 8.4 m (Y) × 70 m (Z), with the partition wall consisting of three diaphragm walls (0.8 m (X) × 16 m (Y) × 18 m (Z)) as shown in Fig. 1 and Fig. 2. Meanwhile, field test method is applied to verify the effect of the control measure.

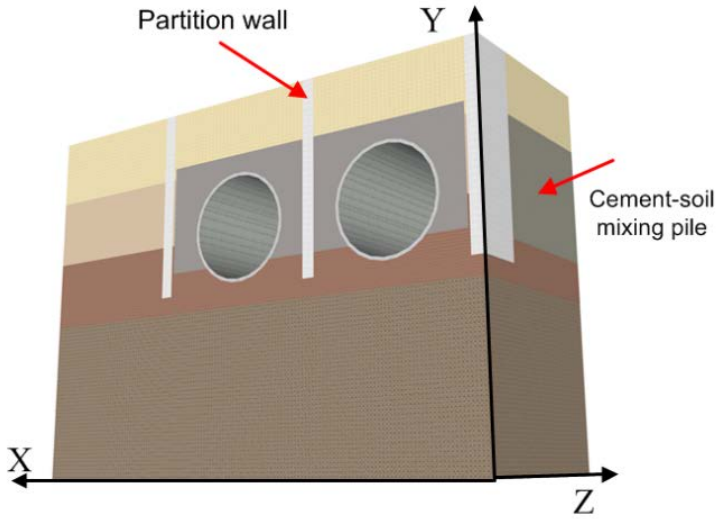

Figure 2. Diagrammatic sketch of the control measure in field.

2.3. Three-dimensional Finite Element Model

A typical three-dimensional numerical model is established by using ABAQUS [34] software. To reduce the boundary effect, the model is 80 m (X) × 40 m (Y) × 40 m (Z) (Fig. 3), consisting of 155,596 elements. Therefore, a complete three-dimensional finite element model considering soil, segment lining, shield, connection bolts and grouting is established.

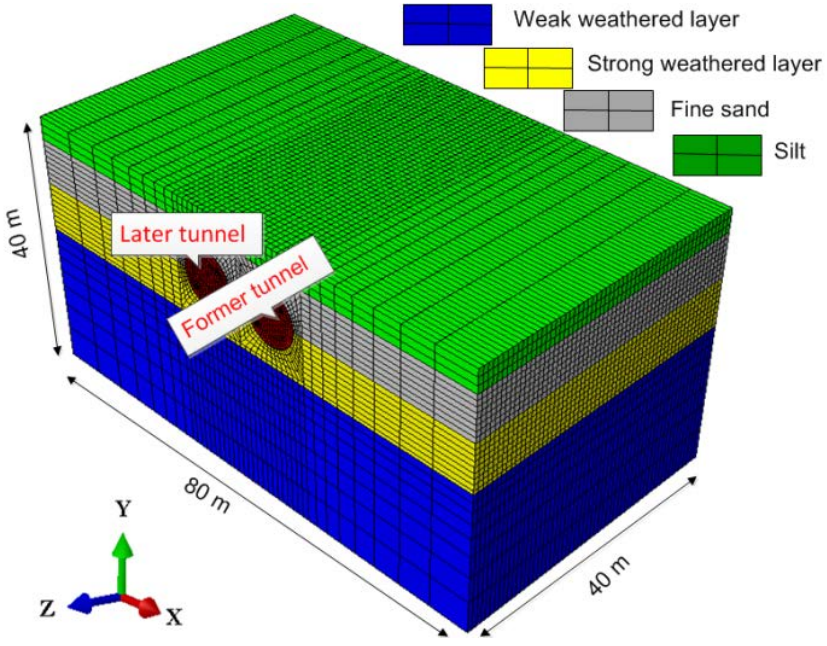

Figure 3. Three-dimensional numerical model.

In view of the discontinuous deformation of the segmental lining, the discontinuous contact model is established for segments of the first excavated tunnel (see Fig. 4), and the remaining lining is assumed to be an equivalent homogeneous structure. Among them, the discontinuous contact model of the segment joint applies the coulomb-contact friction model with a friction coefficient of 0.83 (same as the rubber gasket) [28, 40]. Moreover, the connection bolt between different segments is simulated by beam element (B31) with embedded method, and stagger-jointed assembling method is applied between adjacent segments, same as the actual construction process. For the equivalent homogeneous segments part, the stiffness reduction factor η is 0.746, which is obtained from the equivalent test of discontinuous contact numerical simulation [41].

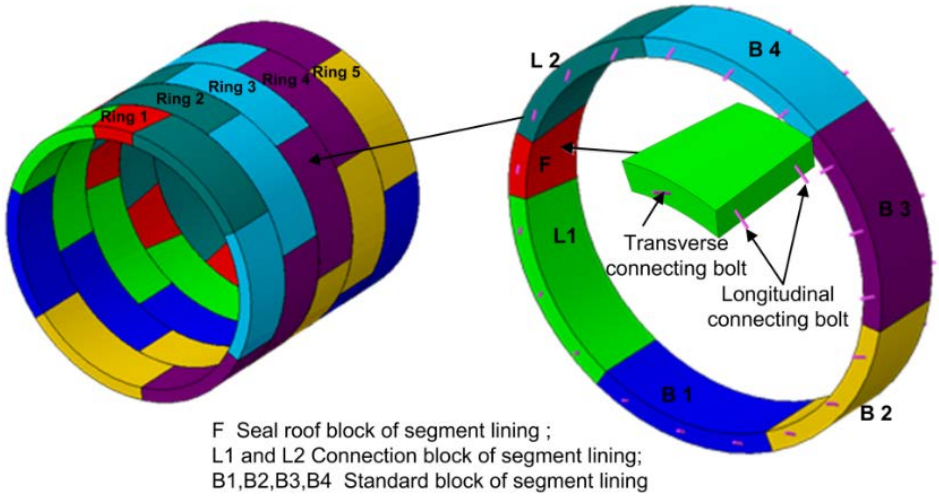

Figure 4. Numerical model of the segment lining.

The shield is simulated by a homogeneous circle with an 8.8 m outer diameter, a 9.6 m length and a 0.15 m thickness. The effect of cutter head and chamber on the excavation surface is equivalent to the soil warehouses pressure and the cutter head torque, as shown in Fig. 5 [35, 37]. Especially, the thickness of the backwall grouting is 0.15 m, and the grouting pressure is simulated by a uniform load of 0.27 MPa [35, 39, 42].

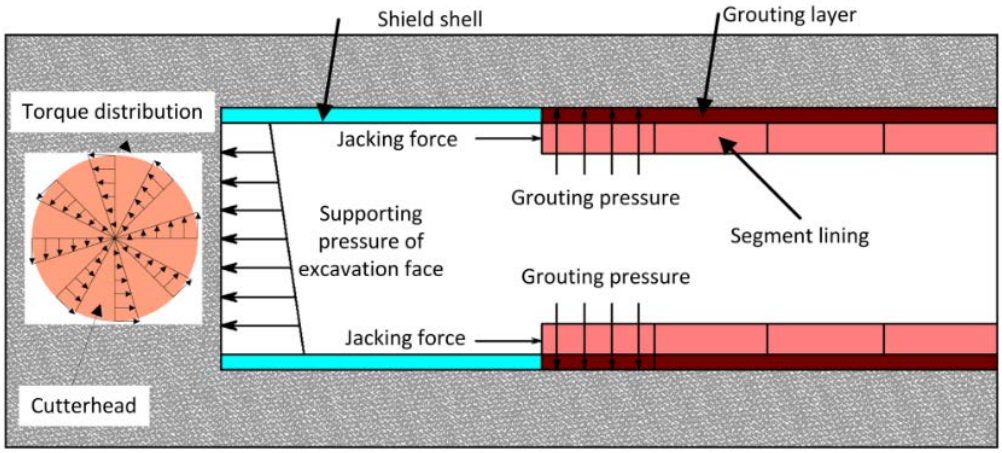

Figure 5. Simulation of the shield tunneling.

For the mechanical boundary, the lateral and bottom surfaces of the numerical model are subjected to normal constraints, and the top surface is a free boundary [5, 7, 8, 28–33, 35]. Soil, segments and shield are simulated by solid elements in the numerical model with C3D8 element. The linear elastic model for isotropic material is used to simulate the segments, shield and connection bolt. And the Mohr-Column model for isotropic material is used to simulate the soil. According to the actual construction sequence, the model change command is used to simulate the tunnel excavation and the assembly process of the segments. The physical properties of materials in the numerical simulation are listed in Table 1.

Table 1. Parameters of the material in the numerical model.

Material	H [m]	ρ [g/cm^3]	E [MPa]	μ	c [kPa]	φ [°]	K_0
Silt	4.5	1.6	10	0.42	10	12	0.45
Fine sand	6.9	1.9	24	0.25	0	26	0.33
Strong weathered layer	8.5	2.0	90	0.39	30	30	0.39
Weak weathered layer	——	2.5	800	0.29	300	38	0.3
Segmental lining(second tunnel)	0.4	2.5	25750	0.2	/	/	/
Segmental lining(first tunnel)	0.4	2.5	34500	0.2	/	/	/
Connecting bolt	——	7.9	206000	0.3	/	/	/
Grouting layer (before hardening)	0.15	1.8	100	0.35	/	/	/
Grouting layer (after hardening)	0.15	2.0	800	0.3	/	/	/

Note: H is thickness; ρ is density; E is modulus; μ is Poisson's ratio; c is cohesion; φ is friction angel; K_0 is lateral pressure coefficient.

3. Results and Discussion

3.1. The Settlement Troughs

First, the settlement troughs determined by the ABAQUS [34] numerical model are analyzed. In general, the settlement trough shape following the Gaussian function may be expected for tunneling in the field condition, for which the symmetrical trough profile about the tunnel center line should exist. Fig. 6 shows transverse settlement trough profiles at ground surface, and after complete passage of the EPB from the control section. It can be seen that the troughs of the ground surface follow Gaussian function. And the ground surface presents a settlement distribution with a single peak after completion of the first tunnel and the maximum settlement is 14.2 mm. In addition, the ground surface presents a settlement distribution with double peaks after completion of the second tunnel; and the maximum settlement is 15.5 mm, which is less than the requirements of standard [43, 44]. As expected [6, 10, 23, 25], the final settlement profiles are asymmetric. This means that the maximum settlement is not on the mid-line between the two tunnels. The shape of the settlement trough is in consistent with that proposed by other researchers [5, 6, 10, 23–25, 30, 36] based on experience in metro engineering worldwide.

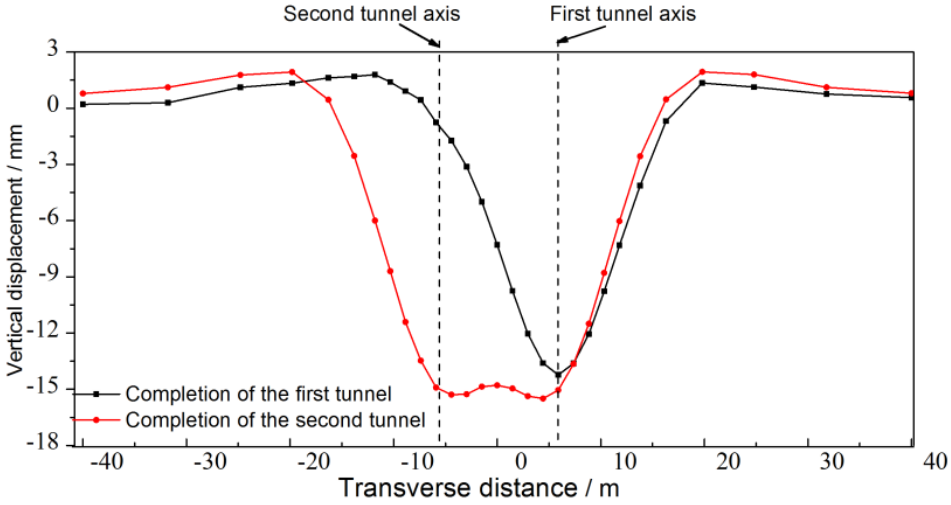

Figure 6. Settlement trough of the ground surface.

Through the comparison of two curves, it can be seen that tunneling of the second tunnel mainly causes the extension of the disturbed area and increases the width of the settlement trough [6, 10, 23, 25]. Moreover, the tunneling of the second tunnel has little influence on the peak value of ground surface trough. This is because the soil sensitivity to the secondary disturbance has been reduced due to the stress release of the soil caused by the construction of the first tunnel.

3.2. Displacement and internal force of the first tunnel

Fig. 7 and Fig. 8 respectively show the total displacement and additional displacement of Ring 3 of the first tunnel. It can be known from the results that the tunnel deformation is symmetrical, and its maximum value is 1.78‰ of the external diameter of segmental lining (D), which satisfies the requirements of standard [43, 44]. The construction of the second tunnel makes the deformation of the first tunnel move away from the second tunnel, resulting in the asymmetric deformation of the segmental lining. A similar rule was found by Kavvadas et al. [28] for tunneling in soft clay.

The seal roof block is in the top region of Ring 3, so that the stiffness of top structure is less than that of the bottom structure [40]. Moreover, as the tunnel passes through the upper-soft and lower-hard stratum, the lower mudstone is stronger than the upper layer, so the upper soil is weaker than lower one in anti-disturbing performance. For this reason, top part of the segment suffers severe displacement than the bottom part.

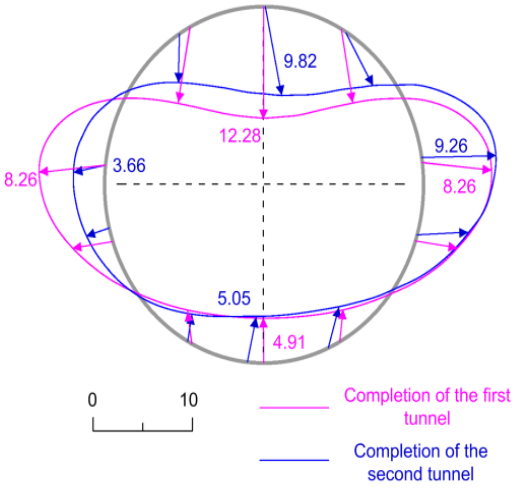

Figure 7. Total displacement of Ring 3 (Unit: mm).

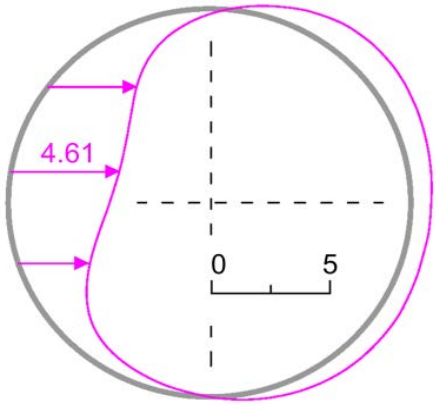

Figure 8(a). Additional horizontal displacement of Ring 3 (Unit: mm).

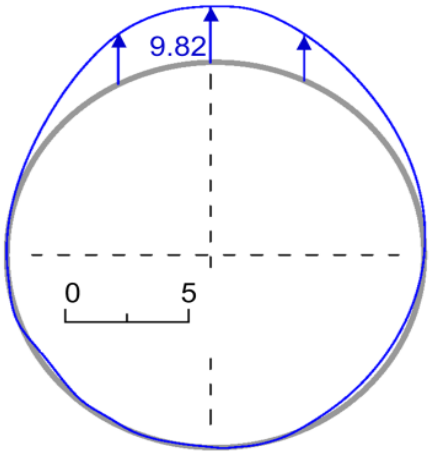

Figure 8(b). Additional vertical displacement of Ring 3 (Unit: mm).

In order to analyze the impact of the second tunnel on the first tunnel, the points (horizontal and vertical) of the maximum additional displacement of Ring 3 are taken as the characteristic points for analysis. The distance between the cutter head and the monitoring section is defined as L. When the cutter head fails to reach the monitoring section of the first tunnel, L is negative. Fig. 9 is the displacement curve at Points A and B of Ring 3. It can be seen that:

I. When $L < -D$ (D is the outer diameter of the shield machine), shear stress and soil warehouses pressure have litter influence on the segments.

II. When $-D < L < 0$, the influence of shear stress and soil pressure is obvious. The deformation rate of the segment increases with the decrease of distance, and the deformation rate reaches peak value once $L = 0$.

III. When 0 < L < D, the deformation of the segment increases with the progress of tunneling and the deformation rate gradually decreases; and the deformation value reaches the peak value when L = D.

IV. When L > D, due to the grouting pressure, the deformation of the segment decreases and will level off finally.

The response of the segment lining significantly increases with the decreasing distance when –D < < L < D. Therefore, this area is the major influenced area and the monitoring of this area should be strengthened during construction.

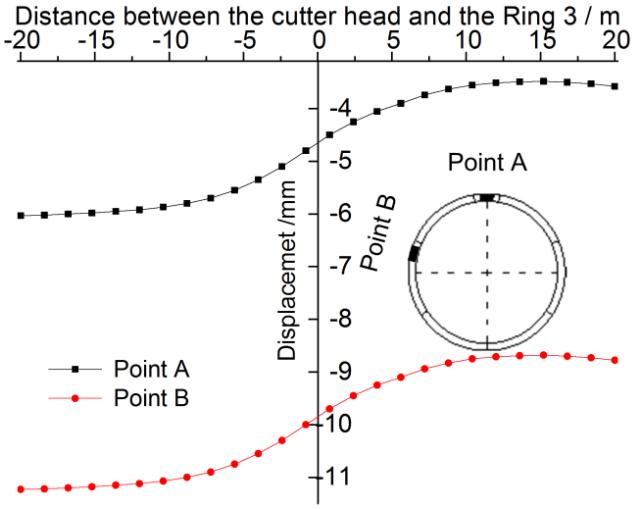

Figure 9. Displacement Curve at Points A and B.

Fig. 10 is a schematic view showing the joint opening of the first lining structure, and Fig. 11 is a curve showing the opening variation of the longitudinal joint in Ring 3.

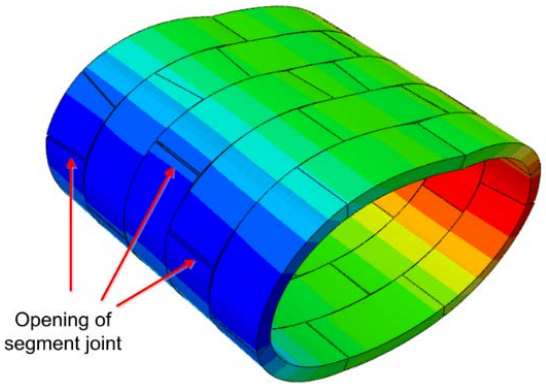

Figure 10. Opening status of the segmental lining.

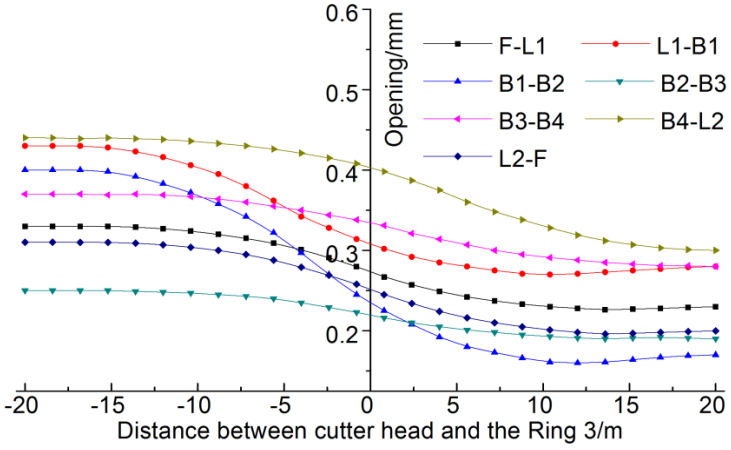

Figure 11. Opening curves of segments in Ring 3.

As shown in Fig. 10, the longitudinal joint opening is obvious, the horizontal joint of the segmental tends to open outwards, and the vertical joint has a tendency to open inside. The hinged action of the bolts provides certain continuity between the segments.

The opening variation of the longitudinal joint in Ring 3 of the first tunnel (Fig. 11) shows that:

I. When L = –20, that is, after completing the construction of the first tunnel, the largest opening of the longitudinal joint is 0.44 mm, which satisfies the requirements [43].

II. When –20 < L < D, the joint opening gradually reduces, which is affected by the lateral loading caused by the construction of the second tunnel.

III. When L > D, the joint opening remains basically unchanged.

The variation law of the joint opening during the construction of the second tunnel is the same as the variation law of the additional deformation of the segment.

Fig. 12 and 13 respectively are the additional stress and maximum principal stress of the segments. Due to the hinge effect of the bolts between the segments, the internal force of the segment is discontinuous at the joint. The maximum tensile stress is 2.44 MPa at the vault region, which exceeds the design value of the tensile strength of C50 concrete (1.89 MPa). Furthermore, the maximum additional tensile stress around the joint area (0.58 MPa) is significantly larger than that in other areas along with longitudinal direction, which exceeds the stress control standard [45, 46].

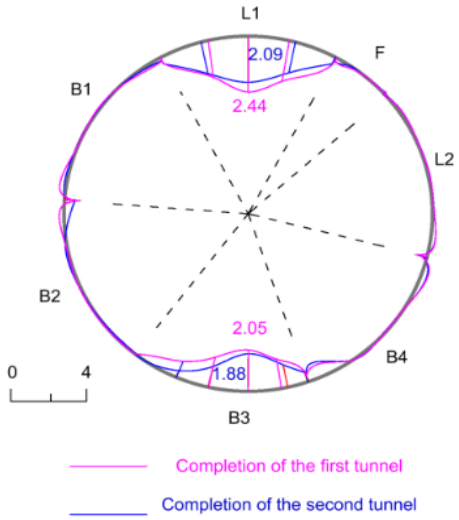

Figure 12. Maximum principal stress distribution of Ring 3 (Unit: MPa).

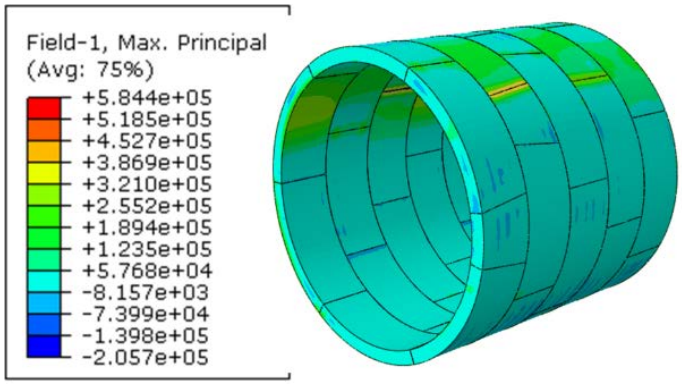

Figure 13. Additional tensile stress distribution of the first tunnel.

3.3. Safety control effect

Fig. 14 and 15 are the maximum principal stress and additional tensile stress contours of the first segments, respectively. It can be seen that after taking safety control measure, the maximum tensile stress of the first segmental lining is 1.7 MPa, smaller than the tensile strength design value of the segmented concrete; the maximum additional tensile stress of the segmental lining is 0.29 MPa, which satisfies the stress control standard [45, 46].

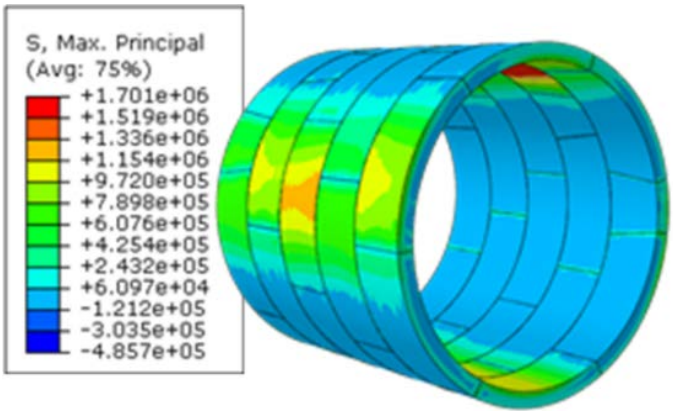

Figure 14(a). The effect of control measure to the first tunnel: Maximum principal stress.

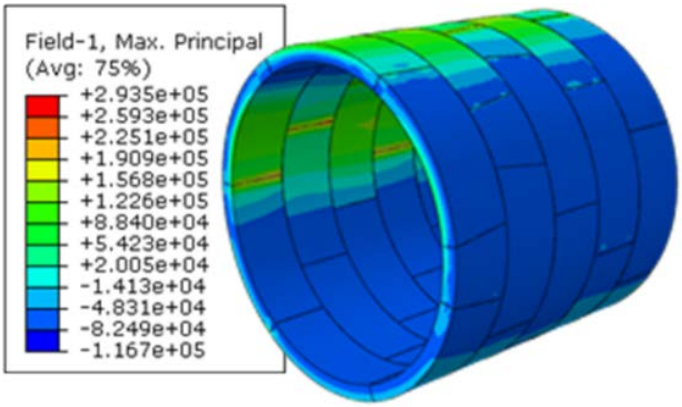

Figure 14(b). The effect of control measure to the first tunnel: Additional tensile stress.

Fig. 15 shows the additional horizontal displacement of the first segmental lining. The maximum additional displacement is 2.43 mm, which meets the requirements of the specification [43, 44].

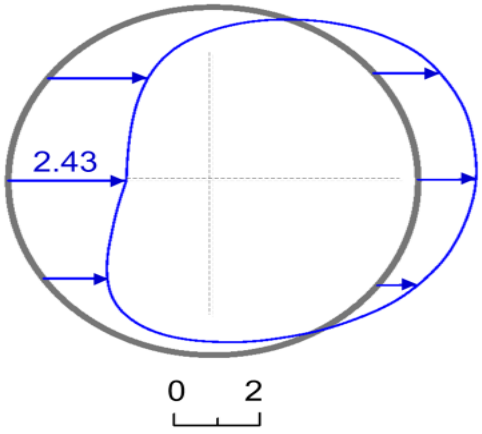

Figure 15(a). Additional horizontal displacement: Filed test results (Unit: mm).

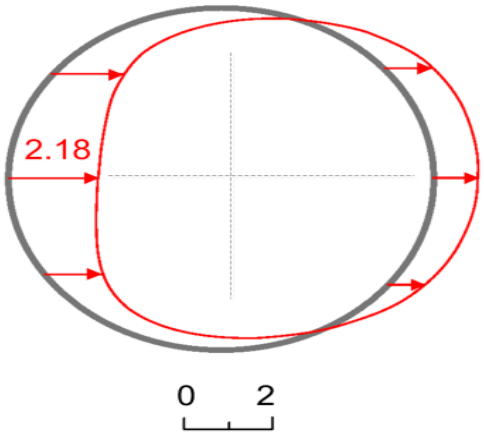

Figure 15(b). Additional horizontal displacement: Numerical results (Unit: mm).

Fig. 16 shows the surface settling trough after taking safety control measure. It can be seen from Fig. 16 that the maximum settlement is 14.16 mm, which can meet the control standard [43, 44]. In addition, the field test is conducted to monitor the settlement of the ground surface. Both the field results and the numerical simulation results are smaller than the control standard, and the law of tested settlement trough and additional horizontal displacement distribution agree with the numerical simulation results. Therefore, conclusions can be drawn that the numerical simulation results are reasonable and reliable, and the pre-reinforcement control measure of partition wall accompanied by cement soil mixing pile is effective.

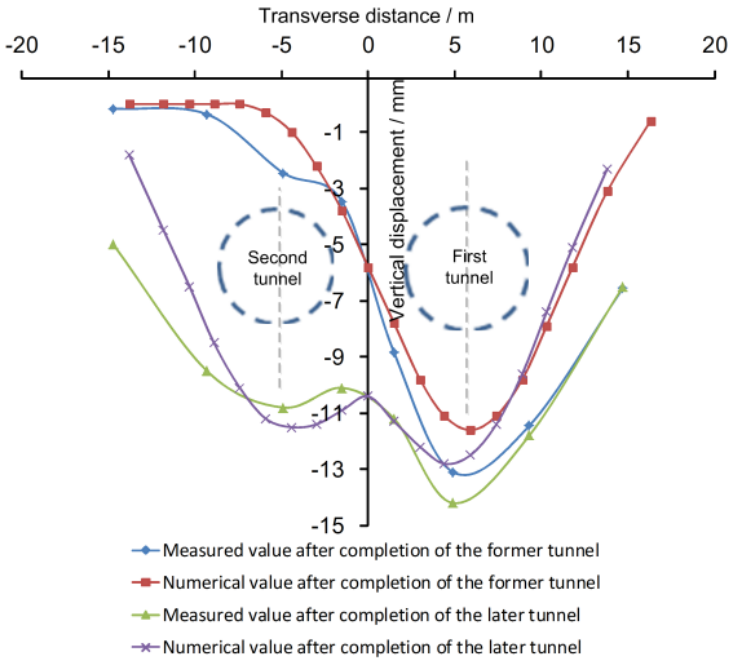

Figure 16. Settlement trough of the ground surface after conducting control measure.

4. Conclusions

This study discusses the interaction and control of shallow-buried twin tunnels with small clear-distance. The following points are outlined as the outcomes of this study.

1. The tunneling process of the new tunnel has a big impact on the stability of the existing tunnel under the condition of shallow burial depth and small clear-distance. The unsafe additional tensile stress 2.44 MPa might be obtained at the vault region, which exceeds the design value of the tensile strength of C50 concrete (1.89 MPa).

2. The seal roof block should not be placed on the top region in cases where the shield tunnel needs to go through the upper-soft and lower-hard composite stratum, the total displacement of the whole ring could be obtained in the seal roof block 12.28 mm.

3. The obviously influenced region of the existing tunnel agrees with the excavation diameter ($-D < L < D$) of the new tunnel, so monitoring in this region should be strengthened.

4. This study demonstrates that the stability of designed structure cannot be ensured and reinforcement is thus required during tunneling. Pre-reinforcement control measure of partition wall accompanied by cement-soil mixing piles has been verified as an effective control method by field tests and numerical results, the maximum settlement could be controlled within 14.16 mm.

5. Acknowledgments

Natural Science Foundation of Jiangsu Higher Education Institutions (No.21KJB560012).

Open Fund of Key Laboratory for Advanced Technology in Environmental Protection of Jiangsu Province (No.JBGS031).

References

1. Jiang, Q., Song, S.G., Li, T., Wang, K., Gu, R.H. Study on surrounding rock stability of small clear-distance twin highway tunnel with eight lanes. Geotechnical and Geological Engineering. 2019. 37(2). Pp. 593–598. DOI: 10.1007/s10706-018-0629-1
2. Hamdy, H.H.A., Enieb, M., Abdelmoamen Khalil, A., Ahmed, A.S.H. Twin tunnel configuration for Greater Cairo metro line. No. 4. Computers and Geotechnics. 2015. 68. Pp. 66–77. DOI: 10.1016/j.compgeo.2015.03.015
3. Lei, M.F., Lin, D.Y., Yang, W.C., Shi, C.H., Peng, L.M., Huang, J. Model test to investigate failure mechanism and loading characteristics of shallow-bias tunnels with small clear distance. Journal of Central South University. 2016. 23(12). Pp. 3312–3321. DOI: 10.1007/s11771-016-3397-1
4. Shi, C., Cao, C., Lei, M. Construction technology for a shallow-buried underwater interchange tunnel with a large span. Tunnelling and Underground Space Technology. 2017. 70. Pp. 317–329. DOI: 10.1016/j.tust.2017.09.009
5. Hage Chehade, F., Shahrour, I. Numerical analysis of the interaction between twin-tunnels: Influence of the relative position and construction procedure. Tunnelling and Underground Space Technology. 2008. 23(2). Pp. 210–214. DOI: 10.1016/j.tust.2007.03.004

6. Fang, Q., Tai, Q., Zhang, D., Wong, L.N.Y. Ground surface settlements due to construction of closely-spaced twin tunnels with different geometric arrangements. Tunnelling and Underground Space Technology. 2016. 51. Pp. 144–151. DOI: 10.1016/j.tust.2015.10.031
7. Do, N.A., Dias, D., Oreste, P., Djeran-Maigre, I. Three-dimensional numerical simulation of a mechanized twin tunnels in soft ground. Tunnelling and Underground Space Technology. 2014. 42. Pp. 40–51. DOI: 10.1016/j.tust.2014.02.001
8. Yang, X.L., Sui, Z.R. Numerical simulation of construction sequence for shallow embedded bias tunnels with small clear distance. Journal of Central South University (Science and Technology). 2007. 38(4). Pp. 764–770.
9. Chen, J.F., Kang, C.Y., Shi, Z.M. Displacement monitoring of parallel closely spaced highway shield tunnels in marine clay. Marine Georesources and Geotechnology. 2015. 33(1). Pp. 45–50. DOI: 10.1080/1064119X.2013.784833
10. Chen, R.P., Zhu, J., Liu, W., Tang, X.W. Ground movement induced by parallel EPB tunnels in silty soils. Tunnelling and Underground Space Technology. 2011. 26(1). Pp. 163–171. DOI: 10.1016/j.tust.2010.09.004
11. Zhang, P., Chen, R.P., Wu, H.N., Liu, Y. Ground settlement induced by tunneling crossing interface of water-bearing mixed ground: A lesson from Changsha, China. Tunnelling and Underground Space Technology. 2020. 96. 103224. DOI: 10.1016/j.tust.2019.103224
12. Huang, F., Ou, R., Li, Z., Yang, X., Ling, T. Limit analysis for the face stability of a shallow-shield tunnel based on a variational approach to the blow-out failure mode. International Journal of Geomechanics. 2018. 18(6). Pp. 04018038. DOI: 10.1061/(asce)gm.1943-5622.0001150
13. Kirsch, A. Experimental investigation of the face stability of shallow tunnels in sand. Acta Geotechnica. 2010. 5(1). Pp. 43–62. DOI: 10.1007/s11440-010-0110-7
14. Boonyarak, T., Phisitkul, K., Ng, C.W., Teparaksa, W., Aye, Z.Z. Observed ground and pile group responses due to tunneling in Bangkok stiff clay. Canadian Geotechnical Journal. 2014. 51(5). Pp. 479–495. DOI: 10.1139/cgj-2013-0082
15. Fu, J., Yang, J., Yan, L., Abbas, S.M. An analytical solution for deforming twin-parallel tunnels in an elastic half plane. International Journal for Numerical and Analytical Methods in Geomechanics. 2015. 39(5). Pp. 524–538. DOI: 10.1002/nag.2322
16. Yang, X.L., Zhang, J.H., Jin, Q.Y., Ma, J.Q. Analytical solution to rock pressure acting on three shallow tunnels subjected to unsymmetrical loads. Journal of Central South University. 2013. 20(2). Pp. 528–535. DOI: 10.1007/s11771-013-1515-x
17. Gong, J., Lei, X., Xia, C. Analysis of field measurement and theoretical calculation on rock pressure in shallow-buried twin tunnels with small spacing. Chinese Journal of Rock Mechanics and Engineering. 2010. 29 (SUPPL. 2). Pp. 4139–4145.
18. Huang, F., Ou, R., Li, Z., Yang, X., Ling, T. Limit Analysis for the Face Stability of a Shallow-Shield Tunnel Based on a Variational Approach to the Blow-Out Failure Mode. International Journal of Geomechanics. 2018. 18(6). Pp. 04018038. DOI: 10.1061/(asce)gm.1943-5622.0001150
19. Ding, W., Liu, K., Shi, P., Li, M., Hou, M. Face stability analysis of shallow circular tunnels driven by a pressurized shield in purely cohesive soils under undrained conditions. Computers and Geotechnics. 2019. 107 (April 2018). Pp. 110–127. DOI: 10.1016/j.compgeo.2018.11.025
20. Chapman, D.N., Ahn, S.K., Hunt, D.V.L., Chan, A.H.C. The use of model tests to investigate the ground displacements associated with multiple tunnel construction in soil. Tunnelling and Underground Space Technology. 2006. 21(3–4). Pp. 413. DOI: 10.1016/j.tust.2005.12.059
21. Lei, M.F., Lin, D.Y., Yang, W.C., Shi, C.H., Peng, L.M., Huang, J. Model test to investigate failure mechanism and loading characteristics of shallow-bias tunnels with small clear distance. Journal of Central South University. 2016. 23(12). Pp. 3312–3321. DOI: 10.1007/s11771-016-3397-1
22. Lei, M., Peng, L., Shi, C. Model test to investigate the failure mechanisms and lining stress characteristics of shallow buried tunnels under unsymmetrical loading. Tunnelling and Underground Space Technology. 2015. 46. Pp. 64–75. DOI: 10.1016/j.tust.2014.11.003
23. Sirivachiraporn, A., Phienwej, N. Ground movements in EPB shield tunneling of Bangkok subway project and impacts on adjacent buildings. Tunnelling and Underground Space Technology. 2012. 30. Pp. 10–24. DOI: 10.1016/j.tust.2012.01.003
24. Zhang, Z.X., Zhang, H., Yan, J.Y. A case study on the behavior of shield tunneling in sandy cobble ground. Environmental earth sciences. 2013. 69(6). Pp. 1891–1900. DOI: 10.1007/s12665-012-2021-4
25. Koukoutas, S.P., Sofianos, A.I. Settlements due to single and twin tube urban EPB shield tunnelling. Geotechnical and Geological Engineering. 2015. 33(3). Pp. 487–510. DOI: 10.1007/s10706-014-9835-7
26. Kirsch, A. Experimental investigation of the face stability of shallow tunnels in sand. Acta Geotechnica. 2010. 5(1). Pp. 43–62. DOI: 10.1007/s11440-010-0110-7
27. Cao, L., Fang, Q., Zhang, D., Chen, T. Subway station construction using combined shield and shallow tunnelling method: Case study of Gaojiayuan station in Beijing. Tunnelling and Underground Space Technology. 2018. 82 (September). Pp. 627–635. DOI: 10.1016/j.tust.2018.09.010
28. Kavvadas, M., Litsas, D., Vazaios, I., Fortsakis, P. Development of a 3D finite element model for shield EPB tunnelling. Tunnelling and Underground Space Technology. 2017. 65. Pp. 22–34. DOI: 10.1016/j.tust.2017.02.001
29. Moeinossadat, S.R., Ahangari, K. Estimating maximum surface settlement due to EPBM tunneling by Numerical-Intelligent approach–A case study: Tehran subway line 7. Transportation Geotechnics. 2019. 18. Pp. 92–102. DOI: 10.1016/j.trgeo.2018.11.009
30. Ng, C.W., Lee, K.M., Tang, D.K. Three-dimensional numerical investigations of new Austrian tunnelling method (NATM) twin tunnel interactions. Canadian Geotechnical Journal. 2004. 41(3). Pp. 523–539. DOI: 10.1139/t04-008
31. Huang, F., Ou, R., Li, Z., Yang, X., Ling, T. Limit Analysis for the Face Stability of a Shallow-Shield Tunnel Based on a Variational Approach to the Blow-Out Failure Mode. International Journal of Geomechanics. 2018. 18(6). Pp. 04018038. DOI: 10.1061/(asce)gm.1943-5622.0001150
32. Li, P., Wang, F., Zhang, C., Li, Z. Face stability analysis of a shallow tunnel in the saturated and multilayered soils in short-term condition. Computers and Geotechnics. 2019. 107 (November 2018). Pp. 25–35. DOI: 10.1016/j.compgeo.2018.11.011
33. Chen, R.P., Tang, L.J., Ling, D.S., Chen, Y.M. Face stability analysis of shallow shield tunnels in dry sandy ground using the discrete element method. Computers and Geotechnics. 2011. 38(2). Pp. 187–195. DOI: 10.1016/j.compgeo.2010.11.003
34. Dassault Simulia International Inc. ABAQUS v 6.4. 2011.

35. Mirhabibi, A., Soroush, A. Effects of building three-dimensional modeling type on twin tunneling-induced ground settlement. Tunnelling and Underground Space Technology. 2013. 38. Pp. 224–234. DOI: 10.1016/j.tust.2013.07.003
36. Fang, Y., He, C., Nazem, A., Yao, Z., Grasmick, J. Surface settlement prediction for EPB shield tunneling in sandy ground. KSCE Journal of Civil Engineering. 2017. 21(7). Pp. 2908–2918. DOI: 10.1007/s12205-017-0989-8
37. Eskandari, F., Goharrizi, K.G., Hooti, A. The impact of EPB pressure on surface settlement and face displacement in intersection of triple tunnels at Mashhad metro. Geomechanics and Engineering. 2018. 15(2). Pp. 769–774. DOI: 10.12989/gae.2018.15.2.769
38. Hilar, M., Tuan, N.T. Evaluation of the surface settlement above the prague metro line an extension constructed by two shields. Acta Polytechnica. 2016. 56(6). Pp. 448–454. DOI: 10.14311/AP.2016.56.0448
39. Shah, R.A., Lavasan, A., Peila, D., Todaro, C., Luciani, A., Schanz, T. Numerical study on backfilling the tail void using a two-component grout. Journal of Materials in Civil Engineering. 2018. 30(3). 04018003. DOI: 10.1061/(ASCE)MT.1943-5533.0002175
40. Wang, S.M., Yu, Q.Y., Peng, B., He, X.F., Yao, J.B. Three-dimensional discontinuous contact model for shield tunnels with double-layer lining based on plastic-damage model. Chin J Rock Mechan Eng. 2016. 35. Pp. 303–311.
41. Li, Y.J. Application of discontinuous contact computational model in mechanical behavior of shield lining. Doctoral dissertation, Beijing Jiaotong University. 2012.
42. Sharghi, M., Chakeri, H., Ozcelik, Y. Investigation into the effects of two component grout properties on surface settlements. Tunnelling and Underground Space Technology. 2017. 63. Pp. 205–216. DOI: 10.1016/j.tust.2017.01.004
43. Ministry of Housing and Urban-Rural Development, People's Republic of China. Code for construction and acceptance of shield tunnelling method. 2017. GB 50446-2017.
44. Ministry of Housing and Urban-Rural Development, People's Republic of China. Code for monitoring measurement of urban rail transit engineering. 2013. GB 50911-2013.
45. Koizumi, A. Design of shield tunnel segments: from the limited state method to the allowable stress method. 2010.

Contacts:

Shouhua Liu, 18945087415@163.com
Yao Shi, 734169065@qq.com
Yiding Zhao, zhaoyiding89@126.com
Rui Sun, 3617384841@qq.com